Structural and Solution Characterization of Mononuclear Vanadium(IV) Complexes That Help To Elucidate the Active Site Structure of the Reduced Vanadium Haloperoxidases

Brent J. Hamstra,[†] Andrew L. P. Houseman,[‡] Gerard J. Colpas,[†] Jeff W. Kampf,[†] Russell LoBrutto,*[,‡] Wayne D. Frasch,*[,‡] and Vincent L. Pecoraro*[,†]

Department of Chemistry, The University of Michigan, Ann Arbor, Michigan 48109-1055, and The Center for the Study of Early Events in Photosynthesis, Department of Botany, Arizona State University, Tempe, Arizona 85287-1601

Received March 13, 1997[⊗]

The complexes [VO(H_2O)ada] (**1**), [VO(H_2O)Hheida] (**2**), and [VO(H_2O)aeida] (**3**) (H_2ada, *N*-(carbamoylmethyl)-iminodiacetic acid; H_3heida, *N*-(2-hydroxyethyl)iminodiacetic acid; H_2aeida, *N*-(2-aminoethyl)iminodiacetic acid) were synthesized and crystallographically characterized. Crystallographic parameters for **1**·2H_2O: monoclinic, space group $P2_1/c$ (No. 14), $a = 7.327(2)$ Å, $b = 23.386(7)$ Å, $c = 7.258(3)$ Å, $\alpha = 90°$, $\beta = 110.95(2)°$, $\gamma = 90°$, $V = 1204.6(7)$ Å^3, $Z = 4$, $R1 = 0.0353$, and $wR^2 = 0.0848$. Crystallographic parameters for **2**·H_2O: orthorhombic, space group *Pbca* (No. 61), $a = 10.512(2)$ Å, $b = 11.727(2)$ Å, $c = 16.719(5)$ Å, $\alpha = 90°$, $\beta = 90°$, $\gamma = 90°$, $V = 2060.6(8)$ Å^3, $Z = 8$, $R1 = 0.0297$, and $wR^2 = 0.0758$. Crystallographic parameters for **3**: monoclinic, space group $P2_1/c$ (No. 14), $a = 6.785(1)$ Å, $b = 9.714(2)$ Å, $c = 14.959(2)$ Å, $\alpha = 90°$, $\beta = 95.12(1)°$, $\gamma = 90°$, $V = 982.2(3)$ Å^3, $Z = 4$, $R1 = 0.0298$, and $wR^2 = 0.0762$. In each structure, the tetradentate ligand is disposed so that the tertiary nitrogen is bound *trans* to the vanadyl oxo, and the rest of the donors occupy equatorial coordination positions. In solution, the structural integrity of these compounds is maintained as observed by UV/visible and EPR spectroscopies, and axial ligation by nitrogen is inferred on the basis of ESEEM spectroscopy. The implications of this study with respect to understanding the coordination environment of VO^{2+} in the reduced, inactive form of vanadium bromoperoxidase (VBrPO) are discussed, and it is proposed that significant changes in the coordination environment of vanadium in VBrPO occur upon its reduction, which may provide a plausible explanation for its irreversible inactivation.

Introduction

The roles of vanadium in the biosphere have become the topic of increased study in recent years. Vanadium occurs naturally in amavadin, a compound isolated from the mushroom *Amanita muscaria* and similar species, it is found in high concentrations in ascidians, and it is known to be essential for the function of certain types of nitrogenase and haloperoxidase enzymes.[1] In addition, vanadium ions and their compounds are known to be potent insulin mimics, and as such may find use as alternatives to insulin in the treatment of diabetes.[2]

Vanadium haloperoxidases (VHPOs) are found in a wide variety of marine algae and lichens and catalyze the formation of a number of halogenated organic compounds.[3] The mechanism of these enzymes is believed to involve binding of peroxide to a vanadium(V) ion, followed by halide oxidation and substrate halogenation by the oxidized halogen species.[4] Unlike the more commonly known heme-containing peroxidases, there is no evidence for metal-centered redox activity in the vanadium enzymes.[5]

Recently, a crystal structure determination of a vanadium chloroperoxidase (VClPO) has been reported, and this structure indicates that a histidine imidazole is the sole protein ligand bound to vanadium.[6] This is consistent with earlier X-ray absorption spectra which indicate that the vanadium(V) ion is surrounded by oxygen and/or nitrogen donors.[7] Upon reduction to vanadium(IV) by dithionite, the enzyme is irreversibly inactivated but becomes amenable to EPR and ESEEM (electron spin echo envelope modulation) spectroscopy. An EPR study of the vanadium bromoperoxidase (VBrPO) from *Ascophyllum nodosum* indicated that water is coordinated to the vanadyl ion, and it was suggested that a protonatable histidine, aspartate, or glutamate residue is near the vanadyl ion.[5] The ESEEM spectrum of the same enzyme indicated the presence of an equatorially-bound nitrogen donor to vanadium.[8] X-ray absorption spectra of reduced VBrPO are also consistent with a coordination environment consisting exclusively of nitrogen and oxygen donors.[7]

In addition to the above-described roles of vanadium, the vanadyl ion (VO^{2+}), when artificially introduced into proteins, can be used as a spectroscopic probe of divalent metal sites in enzymes. Whereas Mg^{2+}, Ca^{2+}, and Zn^{2+} are inaccessible by most spectroscopic methods, and Fe^{2+} and Mn^{2+} yield only limited data whose interpretation is often difficult, VO^{2+} provides a wealth of easily obtained, simply interpreted spectroscopic data. Its d^1 electronic configuration allows visible and EPR spectra, which provide information about the ligand field strength, and, indirectly, the identity of the donors to vanadium, to be readily measured. The additivity relationship for the parallel hyperfine coupling constant determined by Chasteen and extended by others enables the prediction of

* Authors to whom correspondence should be addressed.
[†] The University of Michigan.
[‡] Arizona State University.
[⊗] Abstract published in *Advance ACS Abstracts,* September 1, 1997.

(1) Rehder, D. *Angew. Chem., Int. Ed. Engl.* **1991**, *30*, 148.
(2) (a) Shechter, Y.; Karlish, S. J. D. *Nature* **1980**, *284*, 556. (b) McNeill, J. H.; Yuen, V. G.; Hoveyda, H. R.; Orvig, C. *J. Med. Chem.* **1992**, *35*, 1489.
(3) Butler, A.; Walker, J. V. *Chem. Rev.* **1993**, *93*, 1937.
(4) de Boer, E.; Wever, R. *J. Biol. Chem.* **1988**, *263*, 12326.
(5) de Boer, E.; Boon, K.; Wever, R. *Biochemistry* **1988**, *27*, 1629.
(6) Messerschmidt, A.; Wever, R. *Proc. Natl. Acad. Sci. U.S.A.* **1996**, *93*, 392.
(7) Arber, J. M.; de Boer, E.; Garner, C. D.; Hasnain, S. S.; Wever, R. *Biochemistry* **1989**, *28*, 7968.
(8) de Boer, E.; Keijzers, C. P.; Klaassen, A. A. K.; Reijerse, E. J.; Collison, D.; Garner, C. D.; Wever, R. *FEBS Lett.* **1988**, *235*, 93.

S0020-1669(97)00284-X CCC: $14.00

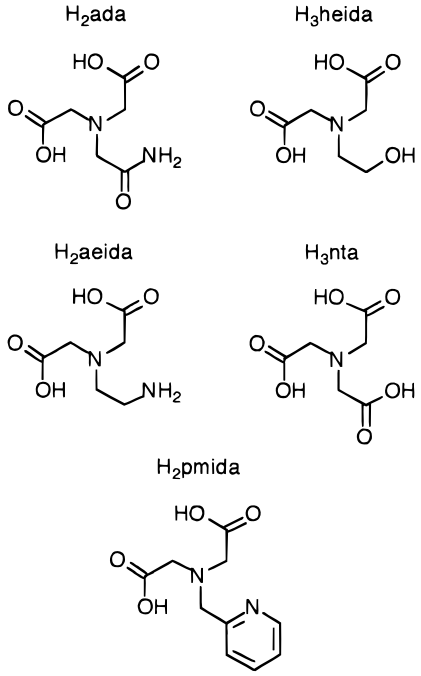

Figure 1. Ligands used in this study.

ligands coordinated in the equatorial plane of the vanadyl ion based on parameters determined for model complexes obtained by varying solution conditions.[9,10]

The vanadyl ion has been probed by continuous wave and pulsed EPR techniques both in naturally occurring vanadoproteins and in vanadyl-substituted systems. A wide variety of vanadyl-substituted proteins have been studied, including pyruvate kinase,[11] *S*-adenosyl methionine synthetase,[12] D-xylose isomerase,[13] apoferritin,[14] lactoferrin,[15] transferrin,[15] and chloroplast F_1-ATPase (CF_1)[16] as well as the reduced form of VBrPO.[8] We are particularly interested in the last two enzymes on this list.

We have recently undertaken a crystallographic and spectroscopic study of a series of vanadyl amino carboxylate complexes in conjunction with our interests in CF_1 and VHPOs. The ligands used are derivatives of iminodiacetic acid (Figure 1), and most of them have been used recently to generate a series of functional models for the VHPOs.[17,18] These ligands include many ligand types that are electronically similar to potential donors to vanadium(IV) in other biological systems as well. The complexes formed are stable in aqueous solution and are readily structurally characterized. The results of this study illustrate the complementary use of crystallography and spectroscopy in determining the structures of vanadyl complexes in aqueous solution, confirm and expand the applicability of the additivity relation in understanding the relationships between the spectra and structures of vanadyl complexes, and suggest a potential reason for the irreversible inactivation of VHPOs upon reduction.

Experimental Methods

The following abbreviations are used throughout the text: H_3nta, nitrilotriacetic acid; H_3heida, *N*-(2-hydroxyethyl)iminodiacetic acid; H_2aeida, *N*-(2-aminoethyl)iminodiacetic acid; H_2ada, *N*-(carbamoylmethyl)iminodiacetic acid; H_2pmida, *N*-((2-pyridyl)methyl)iminodiacetic acid.

H_3nta, H_2ada, 2-picolyl chloride, vanadyl sulfate hydrate, sodium hydroxide, barium hydroxide, *N*,*N*-acetylethylenediamine, bromoacetic acid, vanadyl acetylacetonate, and iminodiacetic acid were purchased from Aldrich Chemical Company. H_3heida was purchased from TCI. Reagent grade acetonitrile was purchased from Mallinckrodt Chemical Co. Ethanol was purchased from McCormick Distilling Co. All chemicals were used as received without further purification.

Synthesis of Compounds. H_2aeida was prepared by the method of McLendon *et al.*[19] Ba[VO(H_2O)nta]$_2$ (Ba[**4**]$_2$) was prepared by the method of Nishizawa and Saito.[20] [VO(H_2O)pmida]·2H_2O (**5**·2H_2O) was prepared by the method of Ooi *et al.*[21] The synthesis of **2** by a different method was independently reported while this manuscript was in preparation.[22]

[VO(H_2O)ada]·2H_2O (1·2H_2O), [VO(H_2O)Hheida]·H_2O (2·H_2O), and [VO(H_2O)aeida] (3). The appropriate ligand [H_2ada (10 mmol, 1.90 g), H_3heida (10 mmol, 1.77 g), or H_2aeida (10 mmol, 1.76 g)] and Ba(OH)$_2$·8H_2O (10 mmol, 3.15 g) for **1** and **2** or NaOH (10 mmol, 0.40 g) for **3** were added to 25 mL of H_2O. The solution was heated and stirred for $^1/_2$ h to dissolve the compounds. To the resulting solution was added vanadyl sulfate hydrate (10 mmol, 2.17 g), and the mixture was heated and stirred for another $^1/_2$ h. The suspension was filtered while warm to remove solids, and the filtrate was allowed to cool. Crystals were obtained upon cooling of the solution and slow evaporation of solvent.

Anal. Calcd (found) for $C_6H_{14}N_2O_9V$ (**1**·2H_2O): C, 23.31 (23.41); H 4.56 (4.48); N 9.06 (9.01). Yield: 53%. UV/visible spectrum (H_2O, pH 5) (λ (nm) (ϵ (M^{-1} cm^{-1}))): 785 (23), 611 (13), 341 (sh) (25). Infrared spectrum (ν, cm^{-1}): 3480, 3326, N−H; 1678, C═O (amide); 1607, C═O (carboxylate); 982, V═O.

Anal. Calcd (found) for $C_6H_{13}NO_8V$ (**2**·H_2O): C, 25.91 (25.84); H 4.71 (4.40); N 5.04 (4.94). Yield: 50%. UV/visible spectrum (H_2O, pH 5) (λ (nm) (ϵ (M^{-1} cm^{-1}))): 824 (23), 621 (9), 341 (sh) (14). Infrared spectrum (ν, cm^{-1}): 3450, O−H; 1612, C═O; 980, V═O.

Anal. Calcd (found) for $C_6H_{12}N_2O_6V$ (**3**): C, 27.81 (27.83); H 4.67 (4.48); N 10.81 (10.66). Yield: 64%. UV/visible spectrum (H_2O, pH 5) (λ (nm) (ϵ (M^{-1} cm^{-1}))): 784 (23), 583 (8), 331 (sh) (29). Infrared spectrum (ν, cm^{-1}): 3300, 3210, 3150, N−H; 1595, C═O; 964, V═O.

Collection and Refinement of X-ray Data. Suitable crystals of compounds **1**−**3** were obtained by the methods described above and mounted in glass capillaries. Intensity data were collected on a Syntex $P2_1$m/v diffractometer using Mo Kα radiation (0.710 73 Å) monochromatized by a graphite crystal whose diffraction vector was parallel to that of the sample. Three standard reflections were measured every 97 reflections. The structures were solved by direct methods and refined by full-matrix least-squares minimizations on the function $\Sigma w(|F_o^2 - F_c^2|)^2$. Hydrogen atoms were located on a difference Fourier map and individually allowed to refine isotropically. All calculations were carried out by the SHELXTL PLUS and SHELXL-93 programs on a VAXStation 3500.

Additional information on the data collection and refinement is reported in Table 1 and in the Supporting Information. Selected bond

(9) Chasteen, N. D. In *Biological Magnetic Resonance*; Berliner, L. J., Reuben, J., Eds.; Plenum Press: New York, 1981; Vol. 3, pp 53−119.
(10) Cornman, C. R.; Zovinka, E. P.; Boyajian, Y. D.; Geiser-Bush, K. M.; Boyle, P. D.; Singh, P. *Inorg. Chem.* **1995**, *34*, 4213.
(11) Tipton, P. A.; McCracken, J.; Cornelius, J. B.; Peisach, J. *Biochemistry* **1989**, *28*, 5720.
(12) Zhang, C.; Markham, G. D.; LoBrutto, R. *Biochemistry* **1993**, *32*, 9866.
(13) Dikanov, S. A.; Tyryshkin, A. M.; Hüttermann, J.; Bogumil, R.; Witzel, H. *J. Am. Chem. Soc.* **1995**, *117*, 4976.
(14) Gerfen, G. J.; Hanna, P. M.; Chasteen, N. D.; Singel, D. J. *J. Am. Chem. Soc.* **1991**, *113*, 9513.
(15) Eaton, S. S.; Dubach, J.; More, K. M.; Eaton, G. R.; Thurman, G.; Ambruso, D. R. *J. Biol. Chem.* **1989**, *264*, 4776.
(16) Houseman, A. L. P.; Morgan, L.; LoBrutto, R.; Frasch, W. D. *Biochemistry* **1994**, *33*, 4910.
(17) Colpas, G. J.; Hamstra, B. J.; Kampf, J. W.; Pecoraro, V. L. *J. Am. Chem. Soc.* **1994**, *116*, 3627.
(18) Colpas, G. J.; Hamstra, B. J.; Kampf, J. W.; Pecoraro, V. L. *J. Am. Chem. Soc.* **1996**, *118*, 3469.
(19) McClendon, G.; Motekaitis, R. J.; Martell, A. E. *Inorg. Chem.* **1975**, *14*, 1993.
(20) Nishizawa, M.; Saito, K. *Inorg. Chem.* **1980**, *19*, 2284.
(21) Ooi, S.; Nishizawa, M.; Matsumoto, K.; Kuroya, H.; Saito, K. *Bull. Chem. Soc. Jpn.* **1979**, *52*, 452.
(22) Mahroof-Tahir, M.; Keramidas, A. D.; Goldfarb, R. B.; Anderson, O. P.; Miller, M. M.; Crans, D. C. *Inorg. Chem.* **1997**, *36*, 1657.

Table 1. Structure Determination Summary

	compound		
	[VO(H_2O)ada]·2H_2O (**1**·2H_2O)	[VO(H_2O)Hheida]·H_2O (**2**·H_2O)	[VO(H_2O)aeida] (**3**)
Formula	$C_6H_{14}N_2O_9V$	$C_6H_{13}NO_8V$	$C_6H_{12}N_2O_6V$
fw	309.13	278.11	259.12
cryst color and habit	blue plate	blue rectangular needle	blue cube
cryst system	monoclinic	orthorhombic	monoclinic
space group	$P2_1/c$ (No. 14)	*Pbca* (No. 61)	$P2_1/c$ (No. 14)
Z	4	8	4
a (Å)	7.327(2)	10.512(2)	6.785(1)
b (Å)	23.386(7)	11.727(2)	9.714(2)
c (Å)	7.258(3)	16.719(5)	14.959(2)
α (deg)	90	90	90
β (deg)	110.95(2)	90	95.12(1)
γ (deg)	90	90	90
V (Å^3)	1204.6(7)	2060.6(8)	982.2(3)
d (obs, g/cm^3)	1.686	1.771	1.754
d (calc, g/cm^3)	1.704	1.793	1.753
temp (K)	178(2)	293	293
no. of data	2366	2042	1937
no. of params	220	198	185
X-ray wavelength (Å)	0.710 73	0.710 73	0.710 73
linear abs coeff (μ, cm^{-1})	8.66	9.92	10.23
R [a]	0.0353	0.0297	0.0298
wR^2 [b]	0.0848	0.0758	0.0762
goodness of fit	1.033	1.057	1.090

[a] $R = \sum(||F_o| - |F_c||/|F_o|)$. [b] $wR^2 = [\sum w(F_o^2 - F_c^2)^2/\sum w(F_o^2)^2]^{1/2}$.

Table 2. Selected Bond Lengths (Å) and Angles (deg) for Compounds **1**−**3**

	1	**2**		**3**
V(1)−O(1)	1.601(2)	1.601(2)	V(1)−O(1)	1.600(2)
V(1)−O(2)	2.015(2)	2.019(2)	V(1)−O(2)	2.029(2)
V(1)−O(3)	2.002(2)	1.988(2)	V(1)−O(3)	2.001(2)
V(1)−O(5)	1.994(2)	2.005(2)	V(1)−O(5)	1.983(2)
V(1)−O(7)	2.012(2)	2.066(2)	V(1)−N(2)	2.131(2)
V(1)−N(1)	2.330(2)	2.313(2)	V(1)−N(1)	2.304(2)
O(1)−V(1)−O(2)	101.86(9)	102.82(6)	O(1)−V(1)−O(2)	102.43(8)
O(1)−V(1)−O(3)	102.48(8)	105.04(6)	O(1)−V(1)−O(3)	106.34(7)
O(1)−V(1)−O(5)	106.43(8)	103.68(6)	O(1)−V(1)−O(5)	102.18(7)
O(1)−V(1)−O(7)	95.54(9)	93.74(5)	O(1)−V(1)−N(2)	92.41(8)
O(1)−V(1)−N(1)	172.58(8)	169.38(6)	O(1)−V(1)−N(1)	169.47(8)
O(3)−V(1)−O(2)	86.58(8)	85.66(6)	O(3)−V(1)−O(2)	83.85(7)
O(3)−V(1)−O(7)	93.98(7)	93.74(5)	O(3)−V(1)−N(2)	92.64(7)
O(3)−V(1)−O(5)	150.87(7)	151.24(5)	O(3)−V(1)−O(5)	151.33(6)
O(5)−V(1)−O(2)	84.12(8)	86.43(6)	O(5)−V(1)−O(2)	87.23(7)
O(5)−V(1)−O(7)	86.80(7)	86.55(5)	O(5)−V(1)−N(2)	89.07(7)
O(2)−V(1)−O(7)	162.05(7)	164.12(6)	O(2)−V(1)−N(2)	165.15(8)
O(2)−V(1)−N(1)	85.28(8)	87.80(5)	O(2)−V(1)−N(1)	88.09(7)
O(3)−V(1)−N(1)	75.67(7)	75.53(5)	O(3)−V(1)−N(1)	75.02(6)
O(5)−V(1)−N(1)	76.09(7)	76.57(5)	O(5)−V(1)−N(1)	77.50(6)
O(7)−V(1)−N(1)	77.51(7)	76.72(5)	N(2)−V(1)−N(1)	77.07(7)

lengths and angles for the compounds are given in Table 2, and complete listings for all compounds are contained in the Supporting Information.

EPR and ESEEM Measurements. CW-EPR experiments were carried out at X-band (9.5 GHz) using a Bruker 300E spectrometer and a liquid nitrogen flow cryostat operating at 100 K. Simulations of the CW-EPR spectra employed the program QPOWA.[23,24] The complexes were dissolved in 50% (v/v) water/glycerol solution to a concentration of 1 mM, and spectra were measured at the pH values indicated in the text.

ESEEM spectra were obtained on a lab-built pulsed spectrometer, with a microwave bridge of standard design, operating at 8.8−9.0 GHz. Pulse timing was controlled by a Macintosh IIci computer, using National Instruments A/D and GPIB control hardware, and Stanford Research Systems DG535 digital delay generators, all programmed via the National Instruments LabView software package. The instrument employs a 50 W pulsed traveling wave tube amplifier, and a one-loop, two-gap resonator made of copper foil which is mounted on the "hourglass" quartz sample tube holder of an APD Cryogenics LTR liquid helium flow cryostat.[25] The cryostat is enclosed in a cylindrical brass shield which is coupled to an X-band waveguide via an oversized iris. Sample tubes are approximately 4.1 mm o.d. × 3 mm i.d.

The spectra shown herein were obtained exclusively from the "stimulated echo" sequence[26] of three $\pi/2$ pulses, each 18−20 ns in duration. Temperatures of 25−30 K and a pulse repetition rate of 1000 Hz were employed. Unwanted echoes were removed from the time-domain spectra by use of the standard, four-part phase cycle.[27] Spectra consisted of 1024 points over a time range of 0−10 microseconds, with each point typically being the sum of about 1000 individual echoes. Spin echo decay functions were fitted to, and then subtracted from, time-domain ESEEM spectra. The residual modulation data were then apodized, using a sine bell function to remove edge artifacts due to truncation of the data set, and then Fourier transformed. Frequency-domain spectra were displayed in modulus form.

Other Methods. UV/visible spectra were recorded on a Perkin-Elmer Lambda 9 spectrophotometer. Infrared spectra were recorded from KBr pellets on a Nicolet 60 SX Fourier transform spectrophotometer. Elemental analyses were performed by the University of Michigan Microanalysis Laboratory.

Results

Syntheses. Synthesis of the amino carboxylate complexes generated in this study was readily accomplished in aqueous solution by adding vanadyl sulfate to an aqueous suspension of the barium or sodium salt of the appropriate ligand (generated *in situ*). The choice of barium or sodium as the cation was made based upon the aqueous solubility of the desired complex. While either can be used in all of these cases, sodium is preferred in cases where the complex is prone to coprecipitate with the barium sulfate generated by the reaction.

Description of Structures. The structures of **1** and **3** are shown in Figure 2. The structure of **2** was reported separately during the course of our studies;[22] therefore, we will give an

(23) Maurice, A. M. Ph.D. Thesis, University of Illinois, Urbana, IL, 1980.
(24) Nilges, M. J. Ph.D. Thesis, University of Illinois, Urbana, IL, 1979.
(25) LoBrutto, R.; Smithers, G. W.; Reed, G. H.; Orme-Johnson, W.; Tan, S. L.; Leigh, J. S. *Biochemistry* **1986**, *25*, 5654.
(26) (a) Mims, W. B. *Phys. Rev.* **1972**, *B5*, 2409. (b) Mims, W. B. *Phys. Rev.* **1972**, *B6*, 3543.
(27) Fauth, J.-M.; Schweiger, A.; Braunschweiler, L.; Forrer, J.; Ernst, R. R. *J. Magn. Reson.* **1986**, *66*, 74.

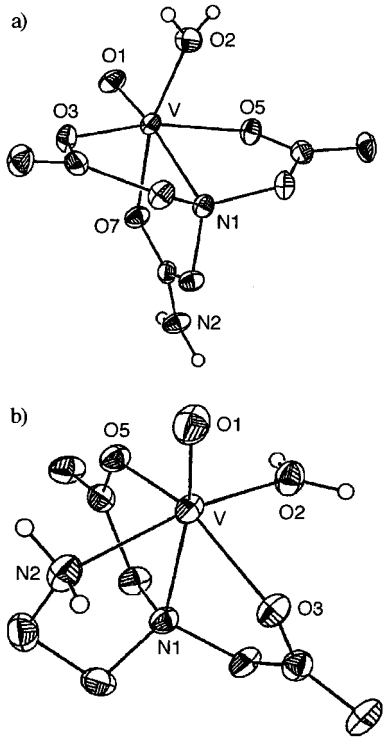

Figure 2. (a) ORTEP diagram of $[VO(H_2O)ada]$ **(1)**. (b) ORTEP diagram of $[VO(H_2O)aeida]$ **(3)**.

abbreviated description herein. Not surprisingly, the three crystal structures obtained show striking similarities. Each exhibits a coordination geometry best described as distorted octahedral. The vanadium−oxo bond lengths V(1)−O(1) determined for the three compounds (1.60 Å) are identical within experimental error and are typical for vanadyl complexes.[21,22,28] In each compound, the tertiary nitrogen of the amino carboxylate ligand is bound *trans* to the oxo moiety of the vanadyl ion. The long V(1)−N(1) distances (2.30−2.33 Å) are a direct consequence of the *trans* influence of the oxo ligand and are similar to the 2.33 Å distance determined for the complex ion $VO(edta)^{2-}$.[28] The oxygen−vanadium−tertiary nitrogen angles are less than the ideal 180° expected (169−173°), as has been observed for the analogous complex $VO(H_2O)$pmida (**5**) (O−V−N angle 172°).[21] As a consequence, the unique donor (carbonyl, alcohol, or amine) in the equatorial region is displaced toward the vanadyl oxygen with respect to the bound water molecule and carboxylate ligands (angles 92−96° vs 102−105° for H_2O and COO^-). The carboxylates are positioned *trans* to each other in the equatorial plane of the vanadyl ion, leaving the unique donor of each ligand situated opposite the bound water molecule. This is in contrast to **5**, in which the carboxylates are *cis* to each other, leaving one *trans* to the water molecule and the other opposite the pyridine donor of this ligand.[21] The carboxylate oxygen−vanadium distances average 2.00 Å, which agree very well with the observed distances found in **5** and $VO(edta)^{2-}$.[21,28] The water oxygen−vanadium bond lengths of 2.015−2.029 Å are also consistent with that observed in **5**.[21] The following paragraphs deal with those structural features unique to the individual complexes.

$[VO(H_2O)ada]\cdot 2H_2O$ ($1\cdot 2H_2O$). This complex exhibits a vanadium−amide carbonyl bond distance of 2.012(2) Å. This distance is only 0.02 Å longer than the average vanadium−carboxylate bond distance in this complex. It appears that the carbonyl oxygen in this case possesses a significant negative charge. Support for this can be found by examining the infrared spectrum of the complex. The observed C═O stretching frequency for the amide carbonyl group of 1678 cm^{-1} is lower in energy when compared to the expected C═O frequency of 1710 cm^{-1}, indicative of a carbon−oxygen double bond weakened by removal of π electron density. These spectroscopic observations are commonly explained by invoking a resonance structure for the amide group in which a negative charge resides on the carbonyl oxygen and a double bond is drawn between the carbonyl carbon and amide nitrogen. In this molecule, the amide C−N bond is 1.307(3) Å, 0.17 Å shorter than the amine C−N bonds, lending additional support for a vital contribution of this resonance form to the nature of the amide moiety.

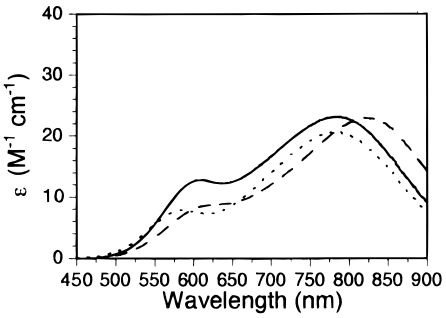

Figure 3. UV/visible spectra of complexes **1**−**3** in aqueous solution (complex concentration = 5 mM) under the conditions described in the text: **1**, solid line (λ_{max}: 785 and 611 nm); **2**, dashed line (λ_{max}: 824 and 621 nm); **3**, dotted line (λ_{max}: 784 and 583 nm).

$[VO(H_2O)Hheida]\cdot H_2O$ ($2\cdot H_2O$). As mentioned above, the structure of this complex has been recently reported by Crans *et al.*[22] Although the structure we obtained is of the water solvate as opposed to the methanol solvate reported by Crans, and the two crystals belong to different space groups, there are no significant differences in the structures of the complexes. The bond from the alcohol oxygen to the vanadium is 2.066(1) Å, which is 0.07 Å longer than the average vanadium−carboxylate bond length in this complex, and 0.05 Å longer than the vanadium−water bond. This bond length is inconsistent with the presence of a significant amount of negative charge on the alcohol oxygen and is to be expected given the clear evidence that the alcohol remains protonated (the alcohol proton, along with all other protons in the lattice, were successfully located and refined). The alcohol proton is hydrogen-bonded to the water molecule of the lattice, which in turn acts as a hydrogen-bond donor toward both oxygens of one of the carboxylates. This may account for the slight difference in bond lengths for the two vanadium−carboxylate bonds.

$[VO(H_2O)aeida]$ (3). The bond between the vanadium and the primary amine nitrogen measures 2.131(2) Å. This bond is 0.05 Å shorter than the corresponding equatorially-bound nitrogen in $VO(edta)^{2-}$.[28] This shorter distance is likely due to the better donor ability of primary amines as compared to tertiary amines. This bond is considerably longer than the bonds to the alcohol and amide carbonyl donors in **1** and **2**, and this series provides yet another clear example of the oxophilic nature of high-valent vanadium ions.

UV/Visible Spectroscopy. Figure 3 shows the UV/visible spectra of complexes **1**−**3** in slightly acidic aqueous solution (pH ≈ 5). Three ligand-field absorption bands are observed in the spectra of these complexes. These transitions are consistent with the tetragonally compressed symmetry commonly associated with spectra of the vanadyl ion and its complexes and can be assigned (from lowest to highest energy) as the $b_2 \rightarrow e_\pi^*$ ($d_{xy} \rightarrow d_{xz},d_{yz}$), $b_2 \rightarrow b_1^*$ ($d_{xy} \rightarrow d_{x^2-y^2}$), and $b_2 \rightarrow a_1^*$ ($d_{xy} \rightarrow$

(28) Nesterova, Y. M.; Anan'eva, N. N.; Polynova, T. N.; Porai-Koshits, M. A.; Pechurova, N. I. *Dokl. Akad. Nauk SSSR.* **1977**, *2*, 350.

Table 3. EPR Parameters, Proposed Equatorial Coordination, and Calculated EPR Parameters Based on Proposed Equatorial Coordination for **1**−**5**

compd	$g_{\|\|}$	$A_{\|\|}$ (exptl), MHz (10^{-4} cm^{-1})	proposed equatorial coord	$A_{\|\|}$ (calcd), MHz (10^{-4} cm^{-1})[a]
1	1.938, 1.936	527 (175.7), 535 (178.3)	[2 $RCOO^-$, 1 $RCONH_2$, 1 H_2O], [1 $RCOO^-$, 1 $RCONH_2$, 2 H_2O]	524 (174.8), 533 (177.8)[b]
2	1.936, 1.933	530 (176.7), 537 (179.0)	[2 $RCOO^-$, 2 H_2O], [1 $RCOO^-$, 3 H_2O][c]	530 (176.8), 539 (179.8)
3	1.9445, 1.942	510.5 (170.2), 518 (172.7)	[2 $RCOO^-$, 1 RNH_2, 1 H_2O], [1 $RCOO^-$, 1 RNH_2, 2 H_2O]	514 (171.2), 523 (174.2)
4	1.939, 1.937	525 (175.0), 532 (177.3)	[3 $RCOO^-$, 1 H_2O], [2 $RCOO^-$, 2 H_2O]	521 (173.8), 530 (176.8)
5	1.943, 1.942	506.5 (168.8), 515 (171.7)	[2 $RCOO^-$, 1 R−N=R′, 1 H_2O], [1 $RCOO^-$, 1 R−N=R′, 2 H_2O]	508 (169.4), 517 (172.4)

[a] Parameters for calculation of $A_{||}$ taken from refs 9 and 10. [b] Parameter for calculation of contribution of $RCONH_2$ to $A_{||}$ taken from that proposed in this work. [c] Parameter for H_2O used as approximation for parameter for ROH.

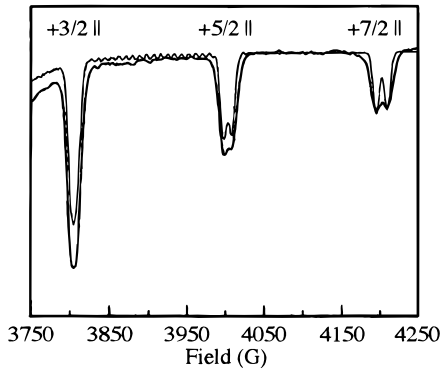

Figure 4. High-field region of the EPR spectrum of **4**. The top spectrum is the simulated spectrum, based on the parameters given in the text; the bottom spectrum is that measured under the conditions described in the text.

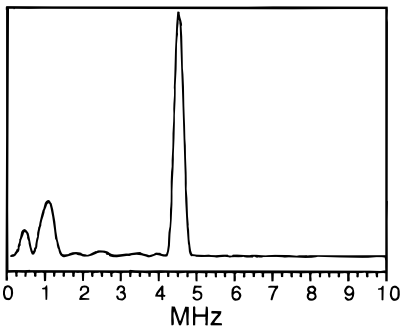

Figure 5. Stimulated-echo ESEEM spectrum (obtained from the $m_I = +^5/_{2\perp}$ EPR transition) of $[VO(H_2O)nta]^-$ **(4)** at pH 4.23. Experimental conditions used: $\nu_e = 9.0201$ GHz; $H_o = 337.7$ mT; $T = 25$ K; $\tau = 190$ ns; pulse train repetition rate = 1200 Hz; each time point represents the sum of approximately 1000 spin echoes.

d_{z^2}) transitions.[29] The value of $10Dq$ can be directly determined from the energy of the $b_2 \rightarrow b_1^*$ transition. The relative positions of this band in the various complexes studied are consistent with what would be expected based on the spectrochemical series (in order of increasing energy, Hheida (R−OH) < ada (R−$CONH_2$) < aeida (R−NH_2)), suggesting that in each case the ligand remains coordinated to vanadium when the complexes are dissolved in water at pH 5. It is notable that the $b_2 \rightarrow b_1^*$ transition for **1** is at very nearly the same energy as that for $[VO(H_2O)nta]^-$ **(4)**.[20] The spectra of the two complexes are sufficiently different to reject amide hydrolysis as a reason for this similarity. Clearly, the amide in this case behaves very much like a carboxylate in terms of its donor ability and ligand field strength.

EPR and ESEEM Studies. We have studied the pH dependence of the UV/visible and EPR spectra of these complexes over a broad pH range, and the results of this extensive study will be reported separately.[30] The EPR spectral data reported here are those which correspond to the pH range at which the complexes are synthesized, and all *trans*-axial ligands remain bound. Table 3 lists, for each of the complexes studied here, the values of $g_{||}$ and $A_{||}$, proposed equatorial ligands, and the calculated $A_{||}$ values derived from the additivity relationship for the proposed ligand sets. EPR spectra and simulations for the complexes studied are contained in the Supporting Information.

$[VO(H_2O)nta]^-$ (4). The EPR spectrum of **4** at pH 4.23 indicates that there are two complexes in solution at this pH. This is easily seen by examination of the portion of the EPR spectrum shown in Figure 4. On the basis of the additivity relationship, the species with the smaller ($A_{||} = 525$ MHz) coupling gives the best fit consistent with a coordination environment in which 3 carboxylates and 1 water molecule are found in the equatorial plane of the vanadyl ion. The coupling for the second species ($A_{||} = 532$ MHz) is consistent with the replacement of one of the carboxylate ligands by a second water molecule. These results are in contrast to the previous study by Micera *et al.*, who reported only one species in solution under these conditions.[31] However, the $g_{||}$ value of 1.937 they report for this species is in agreement with our results, as is their reported value of $A_{||}$ of 176×10^{-4} cm^{-1} (528 MHz), which is roughly the average of the two $A_{||}$ values measured for the two species in the present study.

We have also examined the ESEEM spectrum of this complex under these conditions (Figure 5). Modulation frequencies of 1.0 and 4.5 MHz arising from ^{14}N are observed. This spectrum is markedly different from those previously observed to arise from complexes in which nitrogen donors are coordinated in the equatorial plane of the vanadyl ion, all of which contain frequencies >5 MHz.[12] In the light of the EPR data for this complex, we believe that this relatively weak superhyperfine coupling arises from an axially-coordinated tertiary nitrogen and indicates that there is considerable homology between the crystal structures discussed above and the solution structure of **4**. A thorough treatment of the ESEEM data for this complex and those for other complexes in this study (all of which reveal low-frequency features of this type), including field-dependence studies, simulations of the spectra, and a detailed assignment of the modulations observed, will be the focus of a separate report.[32]

$[VO(H_2O)ada]$ (1). At pH 4.40, this complex also exhibits the same type of EPR spectrum as **4**, with two species apparently present ($A_{||} = 535$ and 527 MHz). The similarity in hyperfine couplings to those of the two species in **4** is noteworthy, as is the fact that the difference in coupling between the two species observed for **1** is identical to that seen for **4**. It is reasonable to

(29) Ballhausen, C. J.; Gray, H. B. *Inorg. Chem.* **1962**, *1*, 111.
(30) Houseman, A. L. P.; Hamstra, B. J.; LoBrutto, R.; Colpas, G. J.; Pecoraro, V. L.; Frasch, W. D. Manuscript in preparation.
(31) Alberico, E.; Micera, G.; Sanna, D.; Dessi, A. *Polyhedron* **1994**, *13*, 1763.
(32) LoBrutto, R.; Hamstra, B. J.; Colpas, G. J.; Pecoraro, V. L.; Frasch, W. D. Manuscript in preparation.

assign the two species as a complex with the tetradentate ligand fully coordinated and one in which a carboxylate or amide carbonyl has been replaced by water. These data are not consistent with amidate nitrogen coordination, as the contribution to $A_{||}$ as reported by Cornman *et al.* for donors of this type results in calculated values of $A_{||}$ that are much smaller than those that are observed for **1**.[10]

Two subtle differences exist between the EPR spectrum of the pair in **1** and of the pair in **4**. First, although there is an 8 MHz difference between the two species within each pair, couplings for the species in **1** are uniformly greater than for **4**, indicating different ligation. Second, whereas the two species in **1** are present in roughly a 1:1 ratio, the species with the larger coupling in **4** is significantly favored over the species with the smaller coupling. These observations suggest that the amide moiety remains coordinated to VO^{2+} in both species and that a carboxylate is displaced by water to form the species with the larger hyperfine coupling.

[VO(H$_2$O)Hheida] (2). As with complexes **4** and **1**, two species are present in the EPR spectrum of **2** at pH 4.78, with hyperfine couplings of 530 and 537 MHz. Since the additivity contribution of a hydroxyl (ROH as opposed to RO^-) moiety is not established, coordination of the Hheida hydroxyl oxygen cannot be ruled out, yielding the possible coordination spheres [1 ROH, 1 H_2O, 2 $RCOO^-$] and [1 ROH, 2 H_2O, 1 $RCOO^-$], respectively, which are consistent with the observations made for **4** and **1** in which only a carboxylate donor appears to be replaced by water. The former ligand set is observed in the crystal structure. The best match between observed hyperfine couplings and those which *can* be predicted from the additivity relation applied to possible sets of ligands is [2 H_2O, 2 $RCOO^-$] and [3 H_2O, 1 $RCOO^-$]. These results are in contrast to the previous study reported by Crans *et al.*, who reported only one species in frozen DMF solution under these conditions.[22] However, the $g_{||}$ value of 1.936 and $A_{||}$ value of 176.7×10^{-4} cm^{-1} (530 MHz) they report for this species are identical to those obtained for the species in which both carboxylates are bound in the present study.

[VO(H$_2$O)aeida] (3). The EPR spectrum of **3** at pH 4.68 again reveals the presence of two species in solution with $A_{||} =$ 510.5 and 518 MHz. This difference again is roughly that expected for water displacement of a single carboxylate, so that the most likely structures in solution have the equatorial coordination [2 $RCOO^-$, 1 RNH_2, 1 H_2O] and [1 $RCOO^-$, 1 RNH_2, 2 H_2O].

[VO(H$_2$O)pmida] (5). As with complexes **1**−**4**, the EPR spectrum of **5** at pH 6.1 reveals the presence of two complexes ($A_{||} =$ 515 and 506.5 MHz) which are consistent with a complex which retains the tetradentate ligand coordination found in the solid state and another species in which water replaces a carboxylate ligand.

Discussion

The chemical complexity of many biomolecules often presents major stumbling blocks in obtaining the detailed structural information that is necessary to understand the activities of these compounds at the molecular level. Spectroscopic methods can provide a solid basis for achieving this understanding. In order to properly interpret spectroscopic data, however, it is vital to be able to discern what types of structural features may give rise to the characteristics of the spectrum measured for the system being studied.

In this respect, small molecules that contain structural features similar to those that may be present in biological systems offer an important contribution to understanding the spectroscopic data obtained from these much more complex molecules. Properly designed model compounds have the advantages that they are frequently much easier to isolate and purify in the laboratory without decomposition or other unwanted chemical modification, do not contain functionalities which may interfere with the observation of the specific properties being studied, are much more amenable to precise structural determination by X-ray crystallography, and are in general more easily studied by spectroscopic means as well. The complexes we have studied here satisfy all of these criteria. With these thoroughly-characterized spectroscopic models, we have a better basis for understanding the EPR spectra of proteins containing the vanadyl ion.

The general principle that each equatorial ligand to VO^{2+} makes an independent contribution to the parameter $A_{||}$ is referred to as "additivity". From the EPR data provided by Chasteen and others on VO^{2+} in a series of aqueous solutions containing potential ligands, it appears that the principle of additivity is quite robust.[9] However, caution must be exercised in using those EPR data alone to identify ligands. Chasteen estimates that the calculated and observed values of $A_{||}$ generally fall within about 3×10^{-4} cm^{-1} (9 MHz) of one another.[9] A discrepancy of this size might occur, for example, if chelate rings in compounds with bi- or tridentate ligands are strained or if other effects distort the square-planar geometry of the equatorial ligands. A second concern is that the model complexes used to assign a specific value of the contribution to $A_{||}$ from each class of ligand may not have the assumed 4-fold symmetry. A bidentate ligand could coordinate asymmetrically, for example, leaving a solvent molecule in the fourth equatorial position. This would introduce an error in estimating the contribution from the bidentate ligand. Finally, such influences as the identity of the axial ligand and the hydrophobicity of the environment (particularly in proteins) could potentially affect contributions to the ^{51}V hyperfine coupling.

We have considered these issues in interpreting the results of the present study. A comparison of $A_{||}$ values obtained from a series of closely analogous model compounds in identical solvent environments is much less error-prone than a *de novo* determination of equatorial ligands to VO^{2+} in a protein environment. Further, the determination of X-ray crystal structures of the model complexes greatly reduces the uncertainty in the set of possible ligands and provides a good indication that the equatorial ligands lie in a plane. A third advantage enjoyed in the present work is the availability of ESEEM for examining the model complexes. This technique can now identify both equatorial and axial coordination by nitrogen.[32] Both ESEEM and X-ray crystallography have been applied to VHPOs as well. Thus, while the extension of the model results to proteins requires care, thorough characterization of the models renders such extension reasonable.

Given these considerations, the synthesis and characterization of compounds **1**−**3** illustrates that crystallography and EPR spectroscopy may be used as complementary techniques for structural determination of vanadium(IV) complexes in much the same way that crystallography and NMR spectroscopy have been used in comparing solid-state and solution structures of vanadium(V) complexes.[33] For these complexes, EPR spectra confirm that the crystallographically determined structures are retained in solution, although in each case there is also a second species with a carboxylate ligand displaced by water that can

(33) (a) Crans, D. C.; Chen, H.; Anderson, O. P.; Miller, M. M. *J. Am. Chem. Soc.* **1993**, *115*, 6769. (b) Crans, D. C.; Shin, P. K. *J. Am. Chem. Soc.* **1994**, *116*, 1305. (c) Colpas, G. J.; Hamstra, B. J.; Kampf, J. W.; Pecoraro, V. L. *Inorg. Chem.* **1994**, *33*, 4669.

be resolved by low-temperature EPR. The equilibrium between these species is unlikely to be observed at room temperature due to the broad line widths common in liquid-phase VO^{2+} EPR spectra.

The knowledge that complexes of this type exhibit close conformity between their solid-state and solution structures allows us to make reasonable predictions about the structure of similar complexes. The crystal structure of **4** has not been reported, although the arrangement of the nta ligand with respect to the vanadyl ion has been inferred from ligand-exchange kinetic experiments, previous EPR studies, and the crystal structure of the mixed-valent $[V_2O_3(nta)_2]^{3-}$ dimer (which bears a strong resemblance to the $[V_2O_3(Hheida)_2]^-$ dimer reported by Crans *et al.*).[20,22,31,34] Our reported structures with analogous ligands lend additional crystallographic support to this hypothesis. The ESEEM spectrum of **4** provides the first direct evidence of coordination by an amine nitrogen in this complex; the low-frequency features observed in this spectrum appear to indicate that the nitrogen is in an axial position with respect to the vanadyl ion. In this case, the characterization of the complex in solution yields a reasonable hypothesis regarding its structure in the solid state. Conversely, the crystal structure of **5** has been reported, whereas the EPR spectrum has not, and the data reported here show that the crystal structure provides a reasonable representation of the solution structure (within a suitable pH range; at extreme pH values such correlations may no longer be justified).

Due to the general agreement between the crystal structures of the complexes and the prediction of equatorial ligands of these complexes in solution using the additivity relationship, the results obtained for **2** are significant. The EPR data appear to indicate that the hydroxyl oxygen, shown to be ligated to vanadium in the crystal structure, is displaced by a water molecule in aqueous solution. However, the proton of the coordinated alcohol was successfully located and refined in the crystal structure of the complex. It is possible that protonation of the coordinated alkoxide group increases the contribution to the hyperfine coupling of this group to a value comparable to that of coordinated water. Support for this hypothesis is found in the EPR data obtained by Crans *et al.*, in which the $A_{||}$ value they report for **2** in DMF solution is identical to one of the two values we report and does not appear to be consistent with the displacement of the hydroxyl group by a DMF solvent molecule (see below).[22]

Of particular interest with respect to the EPR spectroscopy of VO^{2+}-substituted proteins is the fact that the species observed in the EPR spectrum of **1** had larger ^{51}V hyperfine couplings than did those for **4**. This provides additional valuable evidence that the amide moiety can coordinate metals and VO^{2+} in particular. This is not surprising from an inorganic chemistry perspective, but is interesting in the realm of protein biochemistry in which metal-binding sites more frequently contain ligands from the side chains of cysteine (RS^-), lysine (RNH_2), histidine (R═N−R′), tyrosine (Ph−O^-), serine or threonine (ROH), and aspartate and glutamate ($RCOO^-$). Of course, the structures of calmodulin, phospholipase A_2, concanavalin A, and cytochrome *c* oxidase have revealed that oxygens from protein backbone amides do contribute to the coordination spheres of the metals at their binding sites,[35−38] and amide oxygen coordination to copper in stellacyanin has been inferred on the basis of spectroscopic measurements.[39]

The measured ^{51}V hyperfine couplings for **1** also provide a rough measure for the amide oxygen contribution to the coupling that four such equatorial ligands would produce and can help to expand the scale of ligands for use in the additivity relation, as has been done by Cornman *et al.* for amidate nitrogen donors.[10] A single amide appears to increase $A_{||}$ by 3 MHz beyond a single carboxylate. Consequently, we suggest that four amides would increase $A_{||}$ by 12 MHz so that $VO(amide)_4^{2+}$ would have $A_{||} = 524$ MHz (174.7×10^{-4} cm^{-1}). The similarity of the hyperfine couplings of carboxylate and amide complexes with VO^{2+} is consistent with the other observations reported here, namely that there is only a 0.02 Å difference in the V−O bond lengths and that the $b_2 \rightarrow b_1^*$ transition in the UV−visible spectrum is barely perturbed.

Knowledge of the contribution to $A_{||}$ from an amide oxygen has immediate application to the use of the vanadyl ion as a probe of a protein system. In an important regulatory mechanism of CF_1 that minimizes ATPase activity under conditions that do not favor ATP synthesis, Mg^{2+} is known to bind to the catalytic site in a nonfunctional manner. From an analysis of the ^{51}V hyperfine couplings of VO^{2+} bound to a catalytic site of CF_1 under conditions in which the ATPase activity was latent, the best fit of the data was consistent with 1 COO^-, 2 H_2O, and 1 RO^- as equatorial ligands.[40] In the β subunit of the crystal structure of the F_1-ATPase from bovine mitochondria,[41] a carboxylate oxygen from glutamate-188 could become a ligand to the Mg^{2+} at the catalytic site. From the results presented here, we would predict an increase in $A_{||}$ of 3 MHz upon conversion of the analogous glutamate to a glutamine via site-directed mutagenesis of the *Chlamydomonas* chloroplast enzyme. However, the mutation had no effect on $A_{||}$, indicating that this group is not bound to VO^{2+} under these conditions.[42] In contrast, similar EPR analyses of VO^{2+} bound to CF_1 with mutations at aspartate-273 in the β subunit have shown conclusively that this group is ligated to the metal in the latent state.[43]

Examination of Vanadium Bromoperoxidase EPR Spectral Data. The successful use of the additivity relationship in predicting the equatorially coordinated ligands to the vanadyl ion in these complexes and as previously used elsewhere leads us to consider its application to the data obtained and mentioned above for VBrPO from *A. nodosum*. To our knowledge, such an analysis of the data has not been previously reported.

At this point, it is important to note what is known about the types of ligands which may be coordinated to vanadium(IV) in this system. First, coordination by water and/or hydroxide is indicated by the changes in line widths in the EPR spectra of

(34) Nishizawa, M.; Hirotsu, K.; Ooi, S.; Saito, K. *J. Chem. Soc., Chem. Commun.* **1979**, 707.
(35) Babu, Y. S.; Bugg, C. E.; Cook, W. J. *J. Mol. Biol.* **1988**, *204*, 191.
(36) Dijkstra, B. W.; Kak, K. H.; Hol, W. G. J.; Drenth, J. *J. Mol. Biol.* **1981**, *147*, 97.
(37) Reeke, G. N., Jr.; Becker, J. W.; Cunningham, B. A.; Gunther, G. R.; Wang, J. L.; Edelman, G. M. *Ann. N.Y. Acad. Sci.* **1974**, *234*, 367.
(38) Tsukihara, T.; Aoyama, H.; Yamashita, E.; Tomizaki, T.; Yamaguchi, H.; Shinzawa-Itoh, K.; Nakashima, R.; Yaono, R.; Yoshikawa, S. *Science* **1996**, *272*, 1136.
(39) Thomann, H.; Bernardo, M.; Baldwin, M. J.; Lowery, M. D.; Solomon, E. I. *J. Am. Chem. Soc.* **1991**, *113*, 5911.
(40) Houseman, A. L. P.; LoBrutto, R.; Frasch, W. D. *Biochemistry* **1995**, *34*, 3277.
(41) Abrahams, J. P.; Leslie, A. G. W.; Lutter, R.; Walker, J. E. *Nature* **1994**, *370*, 621.
(42) Hu, C.-Y.; Houseman, A. L. P.; Morgan, L.; Webber, A.; Frasch, W. D. *Biochemistry* **1996**, *35*, 12201.
(43) Mutations of aspartate-273 to a histidine, cysteine, and asparagine all caused changes to the EPR spectra of VO^{2+} bound as the VO^{2+}−ATP complex to catalytic site 3 of latent *Chlamydomonas* CF_1. The best fit of the ^{51}V hyperfine parameters of these spectra indicated that, in the histidine mutant, the only change in equatorial ligands from the wild type enzyme was an imidazole nitrogen in lieu of a carboxylate oxygen. Similar results were obtained for the other mutants: Hu, C.-Y.; Houseman, A. L. P.; Frasch, W. D. Unpublished results.

VBrPO in D_2O or $H_2{}^{17}O$, and by the presence of modulations in the ESEEM spectrum attributable to exchangeable protons or deuterons in H_2O and D_2O, respectively.[5,8] Second, the EPR spectrum shows changes with respect to pH consistent with the protonation/deprotonation of a functional group with an apparent pK_a of 5.4.[5] Third, the ESEEM spectrum contains modulation frequencies at 5.3 and 8.1 MHz consistent with equatorial ligation by a histidine imidazole, as opposed to an amine nitrogen, which typically gives frequencies of approximately 4 and 7 MHz.[8,12] Fourth, there is considerable homology between the amino acid sequences of VBrPO and the crystallographically characterized VClPO. This relationship is particularly keen in the regions surrounding the proposed active sites. These regions of the sequence for VBrPO contain several histidine residues, including residues in analogous positions to the vanadium-binding histidine and the proposed acid-base histidine of VClPO, as well as other histidine residues which are not present in VClPO.[6]

Using the average values for $A_{||}$ reported for both the low-pH (166.6×10^{-4} cm^{-1}) and high-pH (159.9×10^{-4} cm^{-1}) forms of the enzyme, and the information given above, the best fits for the equatorial coordination sphere from the additivity relationship given the expected contributions to $A_{||}$ for each donor as reported by Chasteen[9] are [2 H_2O, 1 RO^-, 1 imidazole] ($A_{||} = 167.3 \times 10^{-4}$ cm^{-1}) for the low-pH form and [1 H_2O, 1 OH^-, 1 RO^-, 1 imidazole] ($A_{||} = 160.4 \times 10^{-4}$ cm^{-1}) for the high-pH form. Alternatively, using the lower contribution to $A_{||}$ for "aromatic" imine donors of 38.3 reported by Cornman *et al.*[10] as opposed to the value of 40.7 reported by Chasteen,[9] the best fits are obtained with [2 H_2O, 2 imidazoles] ($A_{||} = 168.0 \times 10^{-4}$ cm^{-1}) for the low-pH form and [1 H_2O, 1 OH^-, 2 imidazoles] ($A_{||} = 161.0 \times 10^{-4}$ cm^{-1}) for the high-pH form. On the basis of EPR data obtained for complexes of the ligand HsalimH (HsalimH: 4-(2-(salicylideneamino)ethyl)imidazole),[44] we believe that Chasteen's value for the contribution to $A_{||}$ may be a somewhat more appropriate parameter for these calculations. More EPR studies of vanadium(IV)−imidazole complexes will likely be necessary to resolve this question. In any event, both of these proposed environments meet the requirements above with respect to the necessity of water-derived ligands, the pH dependence of the spectra (due to the ionization of a bound water molecule; pK_a values for water bound to the vanadyl ion in small molecules have been reported to be ≈ pH 7, and could be lower in a protein environment),[45] and the presence of a histidine imidazole ligand bound to VO^{2+} as indicated by ESEEM.

These assignments are also consistent with the crystal structure of VClPO and its sequence homology with VBrPO.[6] For the first proposal, the equatorially-coordinated imidazole donor may correspond to that coordinated to vanadium(V) in the crystal structure, or possibly an imidazole from a different histidine residue (see below). The alkoxide donor proposed to be bound to vanadium(IV) may arise from any one of a number of serine or threonine residues near the VBrPO active site. One candidate for this ligand is serine-99, which corresponds to serine-402 in the VClPO structure; in this structure this residue is involved in a hydrogen-bonding interaction with the bound vanadate.

Of note is that while the crystal structure of VClPO shows only a single histidine imidazole bound to vanadium, the second structural proposal based on the additivity relationship suggests a second imidazole is also bound. It is possible that this additional ligand derives from the proposed acid/base catalytic histidine residue believed to be present in VBrPO based on the homology with VClPO. Binding of this catalytically essential residue may also explain the inability of the enzyme to be reactivated upon the addition of hydrogen peroxide to reduced VBrPO,[5] since the histidine may play an important role in facilitating the binding of peroxide to vanadium and/or forming the active peroxovanadium oxidizing agent. Alternatively, a significant structural change which prevents reactivation may be caused by the binding of an additional histidine, even if the histidine which is bound is not the acid/base catalyst, but another histidine residue. Such histidine residues are found in the sequence of VBrPO, although they are not found in the VClPO sequence.

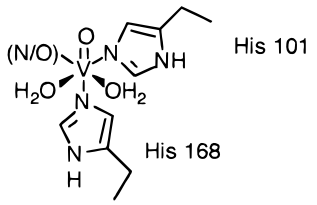

Figure 6. Possible coordination environment of VO^{2+} in reduced VBrPO from *Ascophyllum nodosum* based on the results of this study and the EPR and ESEEM spectra of reduced VBrPO.[5,8] The numbering of histidine residues is based on the homology determined for VBrPO and the vanadium chloroperoxidase as outlined in ref 6. His-101 corresponds to the proposed catalytic histidine His-404 in the chloroperoxidase, and His-168 corresponds to the ligand His-496 in the chloroperoxidase.

Also of note is the similarity of the low-frequency feature at 4.2 MHz in the ESEEM spectrum of VBrPO to the 4.5 MHz feature observed in the ESEEM spectrum of **4**. This feature is believed to arise from an axially-coordinated nitrogen donor in **4**, which lends additional support to the proposition that an additional nitrogen donor may be coordinated to VO^{2+} in reduced VBrPO. It is intriguing to consider that this feature in the spectrum of VBrPO may be due to a histidine located in an axial position with respect to the vanadyl ion. Using the X-ray structure of VClPO as a guide, it is reasonable that the histidine coordinated to vanadium(V) in that structure and an equatorial nitrogen from the proposed acid/base catalytic histidine correspond to the nitrogen modulations detected in the ESEEM spectrum (alternatively, the acid/base histidine may provide the axial ligand and the originally coordinated histidine the equatorial ligand, depending on the alignment of the *z*-axis for the vanadyl ion in this system). A further examination of the possibility of observing axially-bound nitrogen ligands to VO^{2+} is in progress and is, in conjunction with its application to reduced VBrPO and other biological systems, the subject of a separate communication.[32] Figure 6 illustrates a structural proposal for the active site of reduced VBrPO based upon these observations.

Conclusion

We have synthesized and characterized a series of complexes which are spectroscopic models for potential vanadyl-substituted sites in proteins. These studies indicate that crystallography and spectroscopy may be used to complement each other in structural studies of vanadium complexes. Furthermore, our studies have led to a reconsideration of the EPR data obtained for the reduced form of vanadium bromoperoxidase and to the suggestion that significant changes in the coordination environment of vanadium upon reduction may be responsible for the irreversible inactivation of reduced VBrPO. These studies also

(44) Cornman, C. R.; Kampf, J. W.; Lah, M. S.; Pecoraro, V. L. *Inorg. Chem.* **1992**, *31*, 2035.
(45) Saito, K.; Sasaki, Y. *Pure Appl. Chem.* **1988**, *60*, 1123.

suggest an expanded role for EPR and ESEEM spectroscopies of the vanadyl ion in biological systems in understanding its activity as an insulin mimic and also in its use as a spectroscopic surrogate for ions such as Ca^{2+} and Mg^{2+}, since a combination of EPR and ESEEM experiments may yield data both on the type and relative orientation of ligands bound to VO^{2+}.

Acknowledgment. Financial support from the National Institutes of Health (Grant GM 42703) to V.L.P. and the U.S. Department of Agriculture (NRIC Grant 92-01249) to W.D.F. is gratefully acknowledged. We are also grateful to Professor Debbie C. Crans of Colorado State University for kindly allowing us to quote her results prior to publication.

Supporting Information Available: ORTEP figures with complete numbering schemes, tables of crystal data and structure refinement details, fractional atomic coordinates with equivalent isotropic displacement parameters, complete bond distances and angles, anisotropic thermal parameters, and fractional atomic positions for hydrogen atoms for **1**−**3**, and EPR spectra and simulations for **1**−**5** (26 pages). Ordering information is given on any current masthead page.

IC970284X